Ab Initio CBS-QCI Calculations of the Inversion Mode of Ammonia

Daniel J. Rush* and Kenneth B. Wiberg*

Department of Chemistry, Yale University, New Haven, Connecticut 06520-8107

Received: August 13, 1996; In Final Form: November 6, 1996[⊗]

The complete basis set (CBS) extrapolation model chemistry of Petersson and co-workers was used to explore the potential energy surface of the ammonia inversion mode. The CBS-QCI theoretical energies were calculated using 41 points along the inversion surface at the MP2/6-311++G** geometries. A variety of techniques were explored to model the potential surface. Subsequent numerical solution of the one-dimensional Schrödinger equation produced energy levels for ammonia isotopomers in good agreement with experimental transitions. Accounting for the variable nature of the reduced mass with inversion coordinate is shown to be of significance. This study is an important first step in producing reliable methods for making ab initio thermodynamic corrections from ΔE(0 K) to ΔG(298 K) in other nitrogen-containing systems. Because no experimental methods generate data at 0 K, these corrections provide a crucial link between experimental thermochemical energies and ab initio theory.

1. Introduction

The ν_2 normal mode of ammonia[1] has been extensively studied and is a classic example of a symmetric double-minimum potential energy surface (PES).[2] It is of A_1 symmetry and is associated with the "umbrella type" nitrogen inversion motion of the molecule depicted in Figure 1. Here q is the inversion coordinate described in degrees of pyramidalization at nitrogen. Previous work by many groups has shown that the vibrational anharmonicity of nitrogen inversion modes is an important consideration when attempting to understand spectroscopic data. In studies of ammonia isotopomers, Spirko and Kraemer used the nonrigid invertor Hamiltonian method[3] to fit experimental ro-vibrational transitions and obtain anharmonic potential functions and effective geometries for NH_3.[4] In related work, Wormer and co-workers (W-C) have compared the ro-vibrational ν_2 Raman spectrum of NH_3 with an ab initio calculated spectrum at the second-order Møller−Plesset (MP2)[5] level of electron correlation.[6] Calculations of ammonia inversion energy levels directly from ab initio potentials include the work of Wormer as well as that of Bunker, Kraemer, and Spirko (BKS)[7] and that of Campoy, Palma, and Sandoval (CPS).[8]

Each of these studies utilized methods requiring the derivation and definition of a large number of equations specific to the ammonia system. Analytical definitions show up in both the kinetic and potential energy portions of the Schrödinger equation. While these elegant methods take advantage of the high symmetry of the NH_3 molecule, it is difficult to apply the same model to other examples of nitrogen inversion. It is our goal to introduce a general method that can be used to calculate inversion energy levels for many systems without extensive modification of the method or of the computer software.

In this paper we apply the CBS-QCI/APNO ab initio model chemistry of Petersson and co-workers[9] to calculate the nitrogen inversion potential energy surface of ammonia. The kinetic energy terms including the reduced mass function for inversion are calculated from the NH_3 geometries along the inversion coordinate. The one-dimensional, time-independent Schrödinger equation is solved numerically to obtain wave functions and energy levels. Differences between energy levels are then compared to known NH_3 experimental spectroscopic transitions.

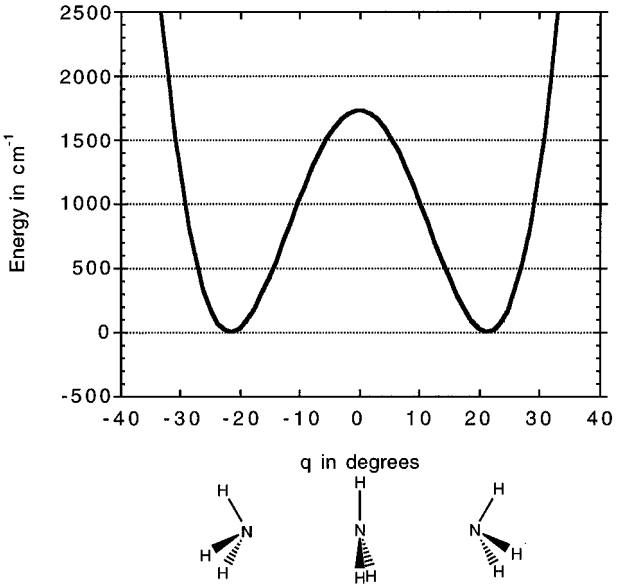

Figure 1. Ammonia inversion potential energy surface showing the umbrella motion.

The importance of nitrogen inversion potential anharmonicity and variable reduced mass is assessed. The FORTRAN programs written for this procedure can be applied to other systems with only minimal alterations.

2. Theory

A. Thermodynamics. Our work on the ammonia molecule was initiated by a problem we encountered during our studies of solvent effects on amide rotational barriers. To compare experimental values to ab initio theory, the calculated energies must be corrected to obtain free energies at temperatures above absolute zero. This requires that the partition function be computed, which is generally separated into translational, rotational, and vibrational components.[10] The vibrational anharmonicity of the NR_2 out of plane wag of amides and the ν_2 nitrogen inversion mode of ammonia complicate the calculation of the vibrational partition function, yet make substantial contributions to the entropy and free energy of the system.

[⊗] Abstract published in *Advance ACS Abstracts,* January 1, 1997.

S1089-5639(96)02435-8 CCC: $14.00

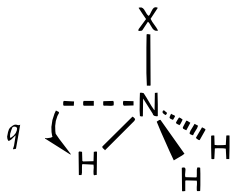

Figure 2. Ammonia inversion coordinate.

Vibrational anharmonicity can be taken into account by excluding the anharmonic modes from the partition function and calculating their thermodynamic contributions separately. We make the assumption that all modes are uncoupled and calculate the input of each to the enthalpy and entropy directly from the vibrational energy levels using the formulas below.[11]

$$H_T^0 - H_0^0 = \frac{N_A \sum_{n=0}^{\infty} \epsilon_n e^{-\epsilon_n/kT}}{\sum_{n=0}^{\infty} e^{-\epsilon_n/kT}} \quad (1)$$

$$S^0 = \frac{H_T^0 - H_0^0}{T} + N_A k \ln\left(\sum_{n=0}^{\infty} e^{-\epsilon_n/kT}\right) \quad (2)$$

Here ϵ_n are the vibrational energy levels referenced to the zero-point energy.

As insufficient experimental data exist to obtain literature values for many nitrogen inversion energy levels, a reasonable alternative is to calculate these properties ab initio. Energy levels for the ammonia inversion mode are solutions to the one-dimensional, time-independent Schrödinger equation below.[12]

$$-\frac{\hbar^2}{2\mu}\frac{d^2\psi(q)}{dq^2} + [V(q) - E]\psi(q) = 0 \quad (3)$$

Here q is the inversion coordinate, μ is the reduced mass appropriate for q, and $V(q)$ is the inversion potential function. The balance of this paper will focus on how ab initio theory may be used to construct and solve this equation for the ammonia molecule to an acceptable level of accuracy.

B. Inversion Coordinate. To define the inversion coordinate, a **Z** matrix was constructed that forced an imaginary atom to maintain equal angles between itself, nitrogen, and the three hydrogens, as depicted in Figure 2. We chose to describe the inversion coordinate q as the amount of pyramidalization occurring at the nitrogen atom, where the value of q is the X−N−H angle minus 90°. This coordinate is adjustable through a single variable, does not enforce C_{3v} symmetry, and is easily adaptable to non-C_{3v} symmetric systems. By using three equal angles as the criterion for placement of the imaginary atom, this definition of q is valid for systems with nonidentical substituents on nitrogen and lower overall symmetry. It also allows a full range of motion for the nitrogen substituents, while permitting easy calculation of the ab initio potential function for any values of q.

C. Potential Function. The ammonia inversion potential surface is a symmetric double well, which is highly anharmonic. An energy barrier to the planar transition state of about 2000 cm^{-1} separates two identical pyramidal minima. This causes a characteristic splitting of the vibrational energy levels into pairs described by symmetric and antisymmetric wave functions. The spacing of these levels is dependent on many parameters of the system including both the height and shape of the central barrier.[2]

Previous investigations have looked at the ammonia energy surface by assuming a functional form for the inversion potential, solving the inverse eigenvalue problem, and fitting to the experimentally observed spectroscopic transitions.[3,4] Ammonia has been especially difficult in that the assumption of the functional form of the potential clearly affects the barrier height and in that the fits to the transitions provide parameters that are seldom unique. The data so obtained may or may not be a "true" representation of the potential energy surface.[13]

Alternatively, ab initio calculation of the inversion potential and subsequent solution of the Schrödinger equation has the advantage of not assuming a priori any functional form for the PES. Once points along the surface have been calculated, they may be fit to a variety of analytical functions or various interpolation methods may be used to fill in the voids. One goal of this study is to determine the best way to handle representing the potential surface in the Schrödinger equation. Another goal is to elucidate the levels of ab initio theory necessary to calculate an inversion surface that can be used to reproduce the experimental transitions of ammonia. Our capacity to reproduce the experimental spectroscopic transitions then becomes a function of our ability to solve the eigenvalue problem and the level of theory with which we can afford to compute the surface.

D. Reduced Mass. The inclusion of a reduced mass (kinetic energy) term in the Schrödinger equation necessitated the selection of a method for its rapid calculation. The lowest energy pathway for ammonia inversion maintains C_{3v} symmetry, but does not keep the N−H bond lengths constant. The derivation of a simple reduced mass expression for this case would be extremely difficult, as the reduced mass actually varies throughout the inversion motion in a path-dependent manner. To be rigorously correct, the reduced mass function that we determine must be the one corresponding to the inversion coordinate q that we have selected. Another consideration in the choice of a method was to ensure that it would be easily adaptable to molecular species without the high symmetry of NH_3.

For the reasons above, we decided to calculate reduced mass using a numerical method. Previously, Laane and co-workers have used a vectorial method to analyze vibrational kinetic energy terms as a function of coordinate.[14] We used identical formulas for the matrix elements, but substituted our ab initio geometries for those determined by vectorial description of the vibrational motion. Durig, using a similar technique, has demonstrated that reduced mass functions calculated from relaxed ab initio geometries can be significantly different from those determined using semirigid vibrational models.[15]

With the fully relaxed atomic positions known as a function of the coordinate, the vibrational−rotational **G** matrix may be determined using equations taken from Laane.[16]

$$\mathbf{G} = \begin{bmatrix} \mathbf{I} & \mathbf{X} \\ \mathbf{X}^t & \mathbf{Y} \end{bmatrix}^{-1} \quad (4)$$

Here, **I** is the 3 × 3 rotational moment of inertia tensor, **X** is a 3 × (3N−6) matrix containing information on vibrational−rotational coupling, and **Y** is a (3N−6) × (3N−6) matrix representing the vibrational contribution. Looking at the inversion vibration alone assumes decoupling from all other vibrational modes and produces the 4 × 4 matrix below designated **G**(q).

$$\mathbf{G}(q) = \begin{bmatrix} \mathbf{I}_{xx} & -\mathbf{I}_{xy} & -\mathbf{I}_{xz} & \mathbf{X}_{11} \\ -\mathbf{I}_{xy} & \mathbf{I}_{yy} & -\mathbf{I}_{yz} & \mathbf{X}_{21} \\ -\mathbf{I}_{xz} & -\mathbf{I}_{yz} & \mathbf{I}_{zz} & \mathbf{X}_{31} \\ \mathbf{X}_{11} & \mathbf{X}_{21} & \mathbf{X}_{31} & \mathbf{Y}_{11} \end{bmatrix}^{-1} \quad (5)$$

While this paper will deal with only a single vibration, it should be noted that this method is a general one. Additional vibrations may be treated by the expansion of the matrix by one row and column per new vibrational coordinate. The matrix elements are defined below where i is the x, y, or z fixed molecular axes, N is the total number of atoms, m_α is the mass of atom α, $\mathbf{r}_\alpha$ is the position vector of atom α relative to the center of mass, and $\mathbf{r}_{\alpha i}$ and $\mathbf{r}_{\alpha k}$ are the ith and kth components of the αth vector.

$$\mathbf{I}_{ii} = \sum_{\alpha=1}^{N} m_\alpha(\mathbf{r}_\alpha \cdot \mathbf{r}_\alpha - r_{\alpha i}^{\,2}) \quad (6)$$

$$\mathbf{I}_{ik} = \sum_{\alpha=1}^{N} m_\alpha r_{\alpha i} r_{\alpha k}, \quad i \neq k \quad (7)$$

$$\mathbf{X}_{ik} = \sum_{N\alpha=1} m_\alpha \left[\mathbf{r}_\alpha \times \left(\frac{\partial \mathbf{r}_\alpha}{\partial q_k}\right)\right]_i \quad (8)$$

$$\mathbf{Y}_{ik} = \sum_{\alpha=1}^{N} m_\alpha \left(\frac{\partial \mathbf{r}_\alpha}{\partial q_i}\right) \cdot \left(\frac{\partial \mathbf{r}_\alpha}{\partial q_k}\right) \quad (9)$$

The matrix can be inverted using standard computer subroutines to obtain a form that is of use to us.[17]

$$\mathbf{G}(q) = \begin{bmatrix} g_{11} & g_{12} & g_{13} & g_{14} \\ g_{21} & g_{22} & g_{23} & g_{24} \\ g_{31} & g_{32} & g_{33} & g_{34} \\ g_{41} & g_{42} & g_{43} & g_{44} \end{bmatrix} \quad (10)$$

This matrix is symmetric about the diagonal. The top left 3 × 3 portion contains purely rotational terms, the upper right and lower left three terms contain the rotational−vibrational coupling, and the lower right corner contains the purely vibrational contribution. For a given position along the coordinate of our single inversion vibration, the reduced mass is determined from the g_{44} term.

$$g_{44} = 1/\mu \quad (11)$$

The $\mathbf{G}(q)$ matrix and the g_{44} term are known to be coordinate dependent for other large amplitude motions.[15,18,19,20] We expected this to be the case with ammonia inversion as well. The $\mathbf{G}(q)$ matrix must be calculated at many positions along the inversion coordinate to enable the calculation of the reduced mass as a function of q.

This method was implemented by a series of FORTRAN programs that were written to utilize the output from our electronic structure calculations. The atomic positions in Cartesian coordinates were translated to a center of mass reference, and the molecule was rotated into the principal axis system. Elements for the $\mathbf{G}(q)$ matrix were calculated using the previously mentioned formulas. The partial derivatives were approximated by taking differences in atomic position for small incremental changes in coordinate q. Subtraction of two ammonia species differing by 0.1° in q was found to be of a good approximation to the derivatives, while retaining sufficient accuracy in the Cartesian coordinates. The reduced mass was mapped as a function of inversion coordinate q and then fit to an eighth-order polynomial in even powers for insertion into the Schrödinger equation. We chose to use an eighth-order polynomial based on literature precedent for using it to model the ammonia PES.[8] While we found it sufficient for use in the kinetic energy portion of the Hamiltonian, its shortcomings for modeling the potential surface will be discussed in section 4.A.

E. Schrödinger Equation. There are some complications introduced into the mathematics of the Schrödinger equation when the reduced mass is included as a function of coordinate. Hougen, Bunker, and Johns (HBJ), in their paper describing the "rigid bender" derivation for triatomics,[21] build upon work summarized by Wilson, Decius, and Cross (WDC)[22] to solve this problem. By looking simply at the large amplitude motion (LAM) vibrational energy levels and assuming the rotational energies in their ground states with quantum numbers, $J_x = J_y = J_z = 0$, HBJ derive the zeroth-order rotational-LAM Hamiltonian below.

$$H_b^0 = -\frac{\hbar^2}{2\mu(q)}\frac{\partial^2}{\partial q^2} - \frac{\hbar^2}{2}\left(\frac{\partial}{\partial q}\frac{1}{\mu(q)}\right)\frac{\partial}{\partial q} - \frac{\hbar^2}{2}|\mathbf{G}(q)|^{1/4}\left\{\frac{\partial}{\partial q}\frac{1}{\mu(q)}\left|\mathbf{G}(q)\right|^{1/2}\left[\frac{\partial}{\partial q}\left|\mathbf{G}(q)\right|^{1/4}\right]\right\} + V(q) \quad (12)$$

Here $|\mathbf{G}(q)|$ is the determinant the $\mathbf{G}(q)$ matrix, and $\mu(q)$ is the reduced mass as a function of the inversion coordinate q. This equation has been simplified by fixing all normal coordinates at their equilibrium values and ignoring the vibrational angular momenta. This effectively holds the small amplitude motions at their equilibrium values while the LAM occurs.[21]

The linear derivative term in (12) may be removed using the substitution

$$\psi_b(q) = \mu(q)^{1/2}\,\phi_b(q) \quad (13)$$

which has the effect of changing the volume element from dq to $\mu(q)$ dq. This provides a Schrödinger equation of the form

$$\frac{\partial^2}{\partial q^2}\phi_b(q) = \left\{f_1(q) + \frac{2\mu(q)}{\hbar^2}[V_0(q) - E]\right\}\phi_b(q) \quad (14)$$

$$f_1(q) = |\mathbf{G}(q)|^{1/4}\,\mu(q)^{1/2}\left\{\frac{\partial^2}{\partial q^2}[|\mathbf{G}(q)^{-1/4}\mu(q)^{-1/2}]\right\} \quad (15)$$

where the $f_1(q)$ term is nearly constant for systems of greater than three atoms.[23] The Schrödinger equation has thus been reduced to its familiar form for a one-dimensional potential, which now includes the reduced mass as a function of LAM coordinate. The wave function ϕ_b must be transformed by eq 13 to give the original wave function ψ_b appropriate for the energy level in question.

As before, the equations are expandable to include multiple vibrational and rotational coordinate dimensions provided the software is written to handle them.[24−26] Complications can arise from the $f_1(q)$ term due to a singularity for linear molecules at $q = 0$, where $f_1(q) = -\infty$. This difficulty was addressed by HBJ, but is not problematic in our case, as $f_1(q)$ either is assumed to be a constant or takes on finite values.

F. Numerov−Cooley Method. Solutions to the one-dimensional Schrödinger equation (14) were obtained for the vibrational energy levels using the Numerov−Cooley[27,28] algorithm implemented in a FORTRAN program.[29] This numerical method was developed to solve second-order differential equations of the form

$$\left[\frac{\mathrm{d}^2}{\mathrm{d}q^2} + Q(q)\right]\psi(q) = 0 \quad (16)$$

TABLE 1: Ammonia Theory Level Dependence (Bond Lengths in Angstroms, q in Degrees, Energy in Hartrees, and ΔE in cm^{-1})

theory level	q_{EQ}	rNH$_{EQ}$	rNH$_{TS}$	E_{EQ}	E_{TS}	ΔE
HF/6-31G*	21.68	1.002 54	0.988 43	−56.184 36	−56.173 99	2276
MP2/6-31G*	22.42	1.016 74	0.999 51	−56.357 38	−56.346 93	2294
MP2/6-31+G*	20.98	1.016 75	1.002 70	−56.366 44	−56.358 64	1751
MP2/6-311++G**	21.49	1.012 73	0.998 18	−56.434 68	−56.426 78	1734
CISD/6-311++G**	21.61	1.011 65	0.996 55	−56.419 76	−56.411 34	1848
CBS-QCI/APNO				−56.559 78	−56.551 57	1802
CBS-QCI/CBSB5				−56.584 45	−56.575 67	1927
lit. ref 38	22.15	1.012 24				

By setting $Q(q) = (2\mu/\hbar^2)[E - V(q)]$, this allows us to solve the Schrödinger equation.

Our implementation utilizes the renormalized Numerov method of Johnson.[30] Combining this algorithm with the work of HBJ, FORTRAN subroutines containing this code were modified to accept the reduced mass as a function of coordinate and transform the wave function back into its original form via eq 13. Subroutines were written to facilitate the search, acquisition, and storage of energy level and wave function data. This was especially useful for cases of symmetric double-well potentials, which can produce nearly degenerate energy levels.[31]

3. Ab Initio Calculations

A. CBS-QCI/APNO Model Chemistry. With the goal of increasing computational performance while reducing cost, Petersson and co-workers have developed the complete basis set (CBS) family of model chemistries.[32] Petersson's highest level method, the CBS-QCI/APNO (complete basis set−quadratic configuration interaction/atomic pair natural orbital) model chemistry,[9] was used to study the inversion potential energy surface of the ammonia molecule. Errors in energy changes and bond dissociation energies using CBS-QCI/APNO are often about half as large as those of Pople's G2 model chemistry.[33] The method is currently limited to about three heavy atoms, which makes it ideal for a high-level calculation of the NH_3 potential surface.

B. Preliminary Calculations. The ammonia molecule and its planar inversion transition state were calculated at several levels of ab initio theory, using the Gaussian program.[34] The results are shown in Table 1 for the C_{3v} equilibrium structure (EQ) and the D_{3h} planar transition state (TS). Diffuse functions are known to be of importance for a good description of lone pair electrons.[35] We expect that they will be especially important in the case of ammonia, where the energy along the inversion coordinate is intimately related to the hybridization of the nitrogen lone pair. Indeed, the addition of a diffuse function on nitrogen at the MP2 level drastically lowers the inversion barrier. In general, it appears that additional diffuse and polarization functions decrease the inversion barrier, while changing the basis set from double to triple ζ or improving the electron correlation treatment increases the barrier.[36] The better levels of theory agree on an inversion barrier just under 2000 cm^{-1} and a shortening of bond lengths of around −0.015 Å in the planar transition state. The 125 cm^{-1} barrier change between the APNO and CBSB5 basis sets is remarkable given the already very sophisticated model at the CBS-QCI/APNO level. This illustrates how difficult it can be to model a "simple" lone pair that undergoes a change in hybridization.

C. MP2/6-311++G Geometries.** For our CBS-QCI calculations along the inversion coordinate we utilized MP2/6-311++G** gradient-optimized geometries. This theory level gives better agreement with ammonia experimental ground state geometry than the QCISD/6-311G** geometry normally used for the CBS-QCI/APNO model chemistry.[37] The 1.0127 Å calculated N−H bond length is very close to the vibrationally averaged bond length determined experimentally at 1.0124 Å.[38] The equilibrium inversion angle at $q_{EQ} = 21.49°$ is also close to the experimental value at $q_{EQ} = 22.15°$. For these reasons, it is also the basis set which Petersson and co-workers have chosen for their CBS-QCI calculations of N−H bond containing species.[37] Mapping the ammonia PES was done at 5° intervals from $q = 0$ to ±60°. This was supplemented by points at 1° intervals from $q = 0$ to ±35° for what will hereafter be referred to as "enhanced" PES calculations. This high density of points was necessary in order to assess the minimum numbers of points needed to accurately interpolate the entire surface. Geometry optimizations in all other degrees of freedom were carried out using tight convergence (maximum force less than 1.5×10^{-4} hartrees/(bohr or radian)). The MP2/6-31++G** optimized geometries every 5° are listed in Table 2.

TABLE 2: Ammonia Geometries along Inversion Coordinate q at the MP2/6-311++G Level of Theory (Bond Lengths in Angstroms, q in Degrees)**

q	rNH	q	rNH
0	0.998 180	35	1.034 393
5	0.999 026	40	1.046 068
10	1.001 521	45	1.062 328
15	1.005 533	50	1.085 006
20	1.010 893	55	1.118 018
25	1.017 452	60	1.168 398
30	1.025 284		

TABLE 3: Calculated Energies at Points along the NH_3 Inversion Potential Energy Surface in Hartrees with q in Degrees[a]

		MP2		CBS-QCI	
q	6-31G*	6-31G*	6-311++G**	APNO	CBSB5
0	−56.173 99	−56.346 93	−56.426 78	−56.551 57	−56.575 67
5	−56.175 13	−56.348 00	−56.427 66	−56.552 44	−56.576 60
10	−56.178 13	−56.350 84	−56.429 95	−56.554 73	−56.579 00
15	−56.181 73	−56.354 36	−56.432 72	−56.557 55	−56.851 95
20	−56.184 15	−56.356 98	−56.434 55	−56.559 56	−56.584 13
25	−56.183 41	−56.356 85	−56.433 84	−56.559 25	−56.584 09
30	−56.177 52	−56.352 13	−56.429 04	−56.555 13	−56.580 44
35	−56.164 64	−56.341 11	−56.419 36	−56.545 81	−56.571 83
40	−56.143 06	−56.322 25	−56.404 40	−56.529 91	−56.556 29
45	−56.111 14	−56.294 23	−56.381 77	−56.505 92	−56.532 06
50	−56.067 27	−56.255 95	−56.348 89	−56.472 26	−56.498 09
55	−56.010 14	−56.206 38	−56.303 91	−56.427 15	−56.452 84
60	−55.939 67	−56.144 12	−56.244 60	−56.368 82	−56.394 53

[a] CBS-QCI calculations utilized the MP2/6-311++G** optimized geometries.

D. Potential Energy Surfaces. Calculations along the inversion potential surface were undertaken with several different levels of ab initio theory, including geometry optimization for all but the CBS-QCI energies. The results for each 5° of q are listed in Table 3 with additional points included in Table S.I of the Supporting Information. Figure 3 illustrates the double-well character of the PES at the MP2/6-31++G** level. At all levels of theory the NH_3 molecule maintains C_{3v} symmetry along the minimum energy pathway. This agrees with experi-

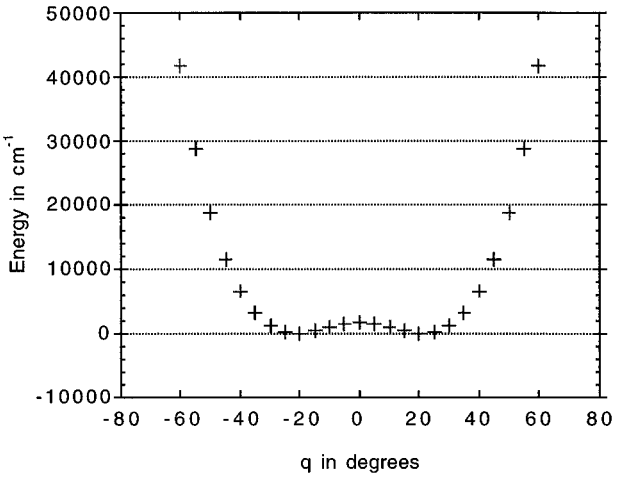

Figure 3. Calculated energies along the ammonia inversion coordinate.

mental observations of A_1 to A_1 vibrational transitions in the Raman experiments of W-C.[6]

Of the two highest level calculations, the first was a QCISD-(T)/6-311++G(2df,p) calculation subsequently corrected by the CBS method of Petersson and co-workers to yield what is known in the literature as the CBS-QCI/APNO energy (without the zero-point correction). The ZPE term included in the CBS-QCI/APNO method was omitted because we calculated the NH_3 inversion potential energy surface at positions away from stationary points. Due to the small size of ammonia, we were able to compute additional energies using the (14s9p4d2f, 6s3p1d)/[6s6p3d2f,4s2p1d] APNO basis set (hereafter known as CBSB5), which was used by Petersson and co-workers in the original formulation of CBS-QCI/APNO.[9a] It is hoped that the diffuse functions in the extended basis set will help to correctly describe the lone pair throughout the inversion coordinate. The combination of the CBS correction with an additional QCISD(T)/CBSB5 calculation represents our highest level of ab initio theory.

E. Reduced Mass $\mu(q)$. Preliminary calculations indicated that the reduced mass is much more sensitive to N−H bond length changes than to angle changes. It is hoped that the MP2/6-311++G** theory level, which gives good bond lengths at the equilibrium geometry, will continue to be accurate at other locations on the potential surface. Calculated values of $\mu(q)$ at 5° intervals along the potential surface for six isotopomers of ammonia are given in Tables S.II, S.III, and S.IV of the Supporting Information with Figure 4 graphing the results for $^{14}NH_3$, $^{14}ND_3$, and $^{14}NT_3$. In all cases, the reduced mass function is a smooth curve that increases in magnitude with distortion from planarity. It does *not* have the double-well shape characteristic of the ammonia PES. As expected, heavier isotopes produce increased masses, with substitution for the hydrogens being more pronounced than changing from ^{14}N to ^{15}N. Substitution of $\mu(q)$ into the Schrödinger equation was facilitated by modeling the reduced mass as an eighth-order polynomial in even powers. The coefficients were determined by fitting to the data from $q = 0$ to 60° using the Levenberg−Marquardt algorithm[39] and are listed in Table 4.

d. Kinetic Energy Term $f_1(q)$. The other kinetic energy term necessary to solve the Schrödinger equation is that known as $f_1(q)$ from the HBJ derivation described earlier. It is a function of inversion coordinate and, like the reduced mass, can be calculated directly from the atomic masses and the geometries along the coordinate via eq 15. The second derivative term was determined by differentiation of an eighth-order polynomial that had also been fit with the Levenberg−

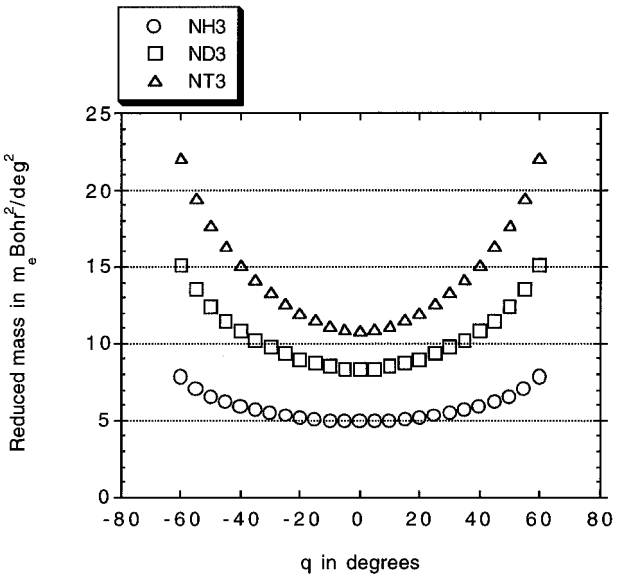

Figure 4. Calculated reduced mass of the ammonia isotopomers along the inversion coordinate.

TABLE 4: Coefficients for $\mu(q) = \mu_0 + \mu_1 q^2 + \mu_3 q^6 + \mu_4 q^8$, Where μ Is the Reduced Mass in m_e bohr^2/deg^2[a]

molecule	μ_0	μ_1	μ_2	μ_3	μ_4
$^{14}NH_3$	4.910	6.669E−4[b]	−7.937E−8	2.089E−11	3.348e−15
$^{15}NH_3$	4.968	6.522E−4	−7.827E−8	2.090E−11	3.347E−15
$^{14}ND_3$	8.334	1.684E−3	−1.578E−7	3.015E−11	8.116E−15
$^{15}ND_3$	8.505	1.640E−3	−1.541E−7	3.011E−11	8.116E−15
$^{14}NT_3$	10.853	2.904E−3	−2.301E−7	3.038E−11	1.396E−14
$^{15}NT_3$	11.145	2.831E−3	−2.259E−7	3.126E−11	1.383E−14

[a] Determined from MP2/6-311++G** optimized geometries using least squares fits to $1/g_{44}$ values at 5° intervals along a ±60° range of q. [b] Read as 6.669×10^{-4}.

Marquardt algorithm to $|\mathbf{G}(q)|^{-1/4}\mu(q)^{-1/2}$ at each point. Values of $|\mathbf{G}(q)|$ and $f_1(q)$ are shown in Tables S.II, S.III, and S.IV of the Supporting Information. The $f_1(q)$ values, which were calculated at 5° intervals, were subsequently fit to another eighth-order polynomial in even powers for substitution into the Schrödinger equation. The coefficients determined for each of the ammonia isotopomers are listed in Table 5, with Figure 5 graphing the results for $^{14}NH_3$, $^{14}ND_3$, and $^{14}NT_3$.

In contrast to the reduced mass, the $f_1(q)$ function *does* have a double-well character for all isotopes examined. The minima of the double well, it should be pointed out, are unrelated to where the minima of the potential energy curve are located. The PES for each species is the same, but the kinetic energy terms have different shapes and characteristic minima. The magnitude of $f_1(q)$ is quite modest in all cases, although it increases with heavy isotope substitution. This agrees with previous work showing that the $f_1(q)$ term is small for molecules with more than three atoms.[23]

4. Inversion Energy Level Calculations

A. Method. Our FORTRAN program provided numerical solutions to the Schrödinger equation via the Numerov−Cooley method when given input for the reduced mass function, the $f_1(q)$ function, and the PES as equation coefficients or data points. Numerically, the integrations were found to converge to ±0.001 cm^{-1} using 2001 points on the inversion coordinate with boundaries set at $q = \pm 70°$. A cubic spline PES interpolation was set to keep $d^2V/dq^2 = 0$ at the end points (natural spline). Calculations of 11 energy levels were complete in under 30 s on a DEC2000 workstation.

TABLE 5: Coefficients for $f_1(q) = a + bq^2 + cq^4 + dq^6 + eq^8$, Where f_1 Is the Additional Hamiltonian Kinetic Energy Term Expressed in Hartrees[a]

molecule	*a*	*b*	*c*	*d*	*e*
$^{14}NH_3$	7.886E−5[b]	−3.403E−7	1.645E−10	−1.999E−14	2.224E−19
$^{15}NH_3$	8.702E−5	−3.516E−7	1.690E−10	−2.092E−14	3.055E−19
$^{14}ND_3$	−2.934E−5	−1.917E−7	1.092E−10	−9.678E−15	−6.011E−19
$^{15}ND_3$	−1.627E−5	−2.097E−7	1.155E−10	−1.069E−14	−5.370E−19
$^{14}NT_3$	−1.173E−4	−6.663E−6	6.587E−11	−3.395E−15	−8.229E−19
$^{15}NT_3$	−1.009E−4	−9.050E−8	7.400E−11	−4.382E−15	−8.333E−19

[a] Determined from MP2/6-311++G** optimized geometries using least squares fit to f_1 values at 5° intervals along a ±60° range of q. [b] Read as 7.886×10^{-5}.

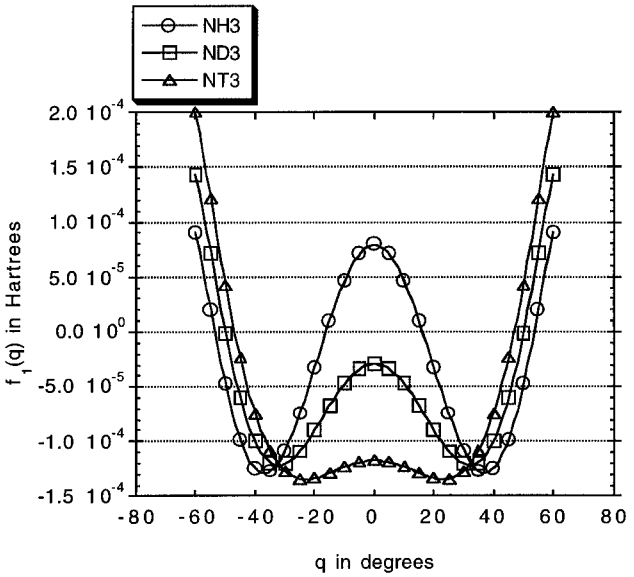

Figure 5. Calculated $f_1(q)$ kinetic energy terms for ammonia isotopomers along the inversion coordinate.

The energy levels are more sensitive to the PES than to the kinetic terms, so we tested various models for their ability to correctly mimic the ab initio ammonia PES. Our results showed the cubic spline interpolation superior to polynomial fits and polynomial interpolation, demonstrating the best propensity to converge with increasing ab initio point density. For all our spline test cases, the difference between points each 5° and each 1° of q was less than 1% in the barrier and 0.2% in energy levels below 5000 cm^{-1}. Polynomial fits are unable to mimic the ammonia PES with sufficient accuracy, even through orders as high as 16th. Although commonly used,[7,8,40,41] the fourth, sixth, and eighth orders underestimate the potential barrier by 445, 220, and 55 cm^{-1}, respectively. We should like to caution against using such low order polynomials for modeling anharmonic potential surfaces.

B. Effect of Potential Surfaces. Table 6 contains the first 11 calculated NH_3 inversional energy levels using increasingly sophisticated ab initio theory to calculate points each 5° of q and utilizing both $\mu(q)$ and $f_1(q)$ at the MP2/6-311++G** level. An example of the output can be seen in Figure 6, which shows the first three pairs of energy levels and their wave functions for ammonia at the CBS-QCI/CBSB5 theory level. One can easily see the tunnel splitting caused by the potential barrier and that the symmetric wave functions are always the lower of the pair in energy.

One of the ways to decrease the expense of calculating potential energy surfaces is to use nonoptimized geometries.[42] The changes in the energy levels caused by holding the N−H bond length constant throughout the inversion at the equilibrium or transition state geometry value can be substantial. Errors over 5% are not uncommon, with some of the low levels moving nearly 100 cm^{-1}, as documented in Table S.V of the Supporting Information. Thus one should be cautious before utilizing this cost saving approximation.

TABLE 6: Values of the Inversional Energy Levels of Ammonia Calculated from the PES at Various Levels of ab Initio Theory in cm^{-1}; Functions for $\mu(q)$ and $f_1(q)$ Calculated at the MP2/6-311++G Level**

		HF	MP2		CBS-QCI	
level	lit.	6-31G*	6-31G*	6-311++G**	APNO	CBSB5
ZPE		575.63	560.54	506.69	501.67	501.71
0+	0.00	0.00	0.00	0.00	0.00	0.00
0−	0.79	0.79	0.55	2.19	1.50	0.99
1+	932.43	1044.94	1025.84	874.96	885.47	905.65
1−	968.12	1082.04	1053.55	951.79	943.94	946.95
2+	1598.47	1792.16	1767.22	1507.70	1515.43	1554.33
2−	1882.18	2102.73	2036.41	1885.33	1858.83	1852.77
3+	2384.17	2664.06	2575.16	2405.17	2367.51	2353.86
3−	2895.61	3235.18	3111.73	2955.61	2903.36	2869.28
4+	3448	3870.29	3714.91	3549.37	3488.46	3440.03
4−	4045	4546.08	4357.21	4175.60	4109.02	4046.79
5+		5259.84	5036.62	4830.65	4762.52	4688.24

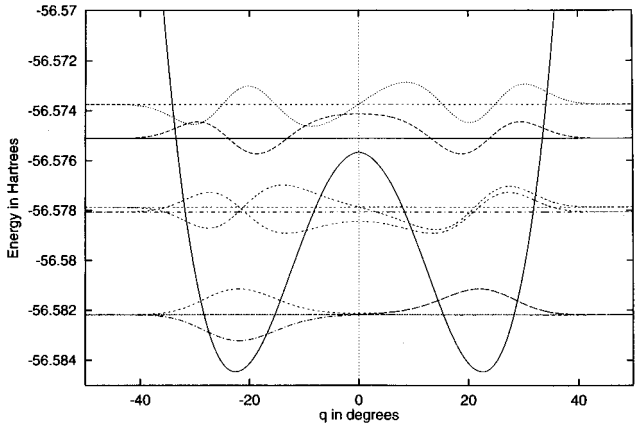

Figure 6. Calculated ammonia inversion energy levels and wave functions.

With the HF/6-31G* PES, the energy levels are calculated about 10% too high in comparison with experiment. The tunnel splittings into symmetric and antisymmetric levels are also a bit too large. The introduction of electron correlation at the MP2 level increases the barrier slightly, which acts to reduce the tunnel splitting. This works in conjunction with the greater effect of correlation decreasing the energetic cost of distortions far from the equilibrium geometry, widening the potential well and lowering all the energy levels.

As one would hope, better ab initio treatments continue to decrease deviation from experiment. The last two columns in Table 6 show the highest levels of theory used. At the CBS-QCI/APNO level the splittings are still a bit too large, but notably, the small CBS correction moves them in the right direction. The CBS modification makes less than a 5 cm^{-1} change in the barrier. Significant improvement is made with the increased basis set of the CBS-QCI/CBSB5 theory level, although it is curious that both the CBSB5 and APNO levels

TABLE 7: Calculated Inversional Energy Levels for Ammonia Isotopomers Compared with Experiment in cm^{-1};[a] Values Determined with the Enhanced CBS-QCI/CBSB5 PES Utilizing $\mu(q)$ and $f_1(q)$ at the MP2/6-311++G Level**

level	$^{14}NH_3$	lit.	$^{15}NH_3$	lit.	$^{14}ND_3$	lit.	$^{15}ND_3$	lit.	$^{14}NT_3$	lit.	$^{15}NT_3$
ZPE	498.11		495.84		379.26		376.48		328.43		325.15
0+	0.00	0.00	0.00	0.00	0.00	0.00	0.00	0.00	0.00	0.00	0.00
0−	0.99	0.79	0.94	0.76	0.06	0.05	0.05	0.05	0.01	0.01	0.01
1+	905.50	932.43	902.45	928.46	726.15	745.60	720.95	739.53	637.12	656.37	631.00
1−	946.84	968.12	942.24	962.89	729.86	749.15	724.33	742.78	637.88	657.19	631.65
2+	1553.20	1598.47	1548.10	1591.19	1327.58	1359.0	1321.01		1205.73		1196.25
2−	1852.91	1882.18	1842.46	1870.86	1399.37	1429.0	1388.41		1226.66		1214.93
3+	2353.99	2384.17	2340.04	2369.32	1790.35	1830.0	1778.47		1625.86		1615.56
3−	2869.27	2895.61	2850.76	2876.13	2067.56	2106.6	2048.55		1782.25		1763.29
4+	3439.37	3448	3416.46		2437.30	2482.0	2413.56		2087.05		2064.33
4−	4046.53	4045	4019.06		2825.38	2876.0	2796.10		2382.78		2353.27
5+	4687.78		4655.65		3243.06		3208.37		2714.21		2678.94

[a] Literature data from ref 3 with none available for $^{15}NT_3$.

give quite good energy levels despite their seeming disparity in calculated barrier heights. Difficulties notwithstanding, our highest level of theory at CBS-QCI/CBSB5 does a very good job at predicting the experimentally observed spectroscopic transitions for NH_3. Of significance is the fact that this procedure does not require fits to the observed energy levels, as all the necessary quantities are calculated from first principles.

C. Comparison with Experiment. For further comparison with experiment, CBS-QCI calculations each 1° of q were run and the resulting enhanced PES data subjected to the previous treatment. The resulting energy levels for six ammonia isotopomers are listed beside the experimental values in Table 7. Overall, the agreement is remarkably good, with the spacing between levels often significantly more accurate than the absolute energies.

There is a consistent underestimation of the energy levels relative to the ZPE. In $^{14}NH_3$ and $^{15}NH_3$ this reaches a maximum of 45 cm^{-1} at the 2+ level and then declines again. In $^{14}ND_3$ it does not seem to have reached the apex by the 4− level. This would seem to suggest that the potential is a bit too wide, especially around the top of the inversion barrier. Relative splittings of the symmetric and antisymmetric levels are slightly too large in most cases except $^{14}NT_3$. Again, where there are enough experimental levels to detect it, the trend seems to be a maximum overestimation near the top of the potential barrier. This would seem to be in the opposite direction from the effect expected from a potential that is too wide, but serves to illustrate that a variety of factors, including a complicated shape dependence on the PES and overall barrier height, are at play. These factors are also at work in the spacings between levels of identical parity, which are underestimated, but show a trend toward overestimation at higher levels.

D. Effect of Reduced Mass. After having established our best level of theory, it is of interest to investigate the effect of changes in the kinetic terms of the Schrödinger equation on the calculated inversion energy levels. Holding reduced mass constant at either the equilibrium or transition state value has a larger effect than calculating the reduced mass function at a lower level of theory. For $^{14}NH_3$, fixing $\mu(q)$ at the planar geometry increases the energy of the 1+ level by 20 cm^{-1} and the 5+ level by 180 cm^{-1}, while complete functions calculated at a lower theory level changed the 5+ level by only 5 cm^{-1}. Fixing $\mu(q)$ at the equilibrium value causes a maximum decrease of about 14 cm^{-1} in the energy levels below 5+. This rather small effect is caused by a favorable bias in the ammonia system. Because the shape of the $\mu(q)$ function is parabolic, while the PES has a double-well shape, the equilibrium value of the reduced mass is a crude average of the values assumed by $\mu(q)$ in a typical inversion motion. In systems like amides, the minimum of the PES coincides with the minimum of the reduced mass function. Using the equilibrium value in such a case would not gain this special benefit of the ammonia system. Data from modification of the reduced mass function are included in Table S.VI of the Supporting Information.

TABLE 8: Comparison of Ammonia Inversion Vibrational Energy Levels Calculated from ab Initio Potentials in cm^{-1}

	this work[a]	W-C MP2[b]	W-C SCF[b]	CPS[c]	BKS[d]	lit.[e]
0+	0.00	0.0	0.0	0.00	0.00	0.00
0−	0.99	0.5	1.3	1.00	1.02	0.79
1+	905.50	1031.2	1023.0	924.12	986.7	932.43
1−	946.84	1071.4	1099.1	981.04	1032.3	968.12
2+	1553.20	1627.4	1661.1	1559.57	1682.0	1598.47
2−	1852.91	1974.9	2086.8	1931.34	2011.6	1882.18
3+	2353.99			2473.40		2384.17
3−	2869.27			3065.91		2895.61

[a] Our highest CBS-QCI/CBSB5 theory level. [b] Wormer and coworkers, ref 6. [c] Campoy, Palma, and Sandoval, ref 8. [d] Bunker, Kraemer, and Spirko, ref 7. [e] Reference 3.

E. Effect of Kinetic $f_1(q)$ Term. The supplementary Table S.VII includes a recalculation of Table 7, where the $f_1(q)$ term has been set equal to zero. The largest change is in the zero-point energy, which decreases for all isotopes. However, the maximum effect is just over 1 cm^{-1} in ZPE and far less for most of the energy level differences. Thus the assumption which can be made to ignore the $f_1(q)$ term is a valid one for ammonia and its isotopomers. We choose to leave it in most of our calculations because it was easily obtained during our calculation of the reduced mass.

F. Comparison with Previous Studies. Ammonia and its isotopomers have been the subject of numerous computational and experimental studies. Of particular relevance to us is work of Spirko and Kraemer, who used an ab initio CISD (13s8p4d,9s3p)/[8s5p3d,6s2p] calculated PES to supplement the input for their nonrigid invertor Hamiltonian method.[4] By using the ab initio potential as a model to adjust their parameters, they fit to the experimental spectroscopic transitions and achieved very close agreement with the observed energy levels. Their best fit indicated a potential barrier of 1884 cm^{-1}, although other fits varied this number by over 90 cm^{-1}. Ab initio theory was used to assist in the fitting of experimental data, and the study stopped short of having the calculations stand alone.

Table 8 shows our results for the first six $^{14}NH_3$ energy levels using our highest levels of theory alongside subsequent columns containing previously published work from other groups and the experimental transition energies. In all these studies the energy levels were calculated directly from ab initio potentials without fits to spectroscopic transitions, although it should be noted that agreement with experiment was never the primary goal of the work.

Bunker, Kraemer, and Spirko (BKS) used CISD calculations with a (11s7p1d,6s1p)/[5s4p1d,3s1p] basis set, fit them to an analytical potential function, and calculated inversional energy levels that were between 5 and 10% too high.[7] This study was concerned with assessing the ability of their analytical function, which they were using in the nonrigid invertor Hamiltonian work, to model the PES of ammonia. Although their work represents the best of the previous computational studies, their potential function was based on an eighth-order polynomial, which we have shown to be a possible source of significant errors. While the theory level of their ab initio calculations was quite good, it seems doubtful that they were able to reach a solid convergence of the energy levels.

Later, Campoy, Palma, and Sandoval (CPS) utilized a numerical method to calculate the energy levels using points from the published potential of BKS.[8] The goal was the development of a mathematical method for solving the Schrödinger equation for very anharmonic potential surfaces.[43] Again, an eighth-order polynomial was used in the PES model. Additionally, the CPS work utilized a constant reduced mass, which is a poor assumption, as previously discussed. The fortuitous agreement with experiment took advantage of the fact that the reduced mass at the equilibrium geometry happens to be an approximate average of its value over the course of the motion. At best, the CPS results should have been no better than those of BKS, whose literature potential they used.

In a more recent study, Wormer and co-workers (W-C) carried out MP2 calculations with a (12s8p3d1f,7s2p1d)/[10s7p3d1f,6s2p1d] basis set.[6] Here, the fairly low level of the correlation treatment might have adversely effected the PES, although they also acknowledge problems in their fitting procedures. The W−C predictions at the SCF level were too high, as we also found using HF potentials. This was improved somewhat by adding electron correlation at the MP2 level, but clearly the lack of a high-level correlation treatment introduced major errors.

In comparison with previous attempts at ab initio prediction of ammonia inversion energy levels, our method performs significantly better. While the others are in error by more than 100 cm^{-1} within the first six levels, our worst error is about 45 cm^{-1}, with most well below that. This would appear to be due to the improvements in the theory level at which we calculated the PES and to the improved method developed to find the energy levels with a high degree of precision.

5. Conclusions

The method we have developed for calculating the inversion energy levels uses a minimum of assumptions and maintains enough generality to be easily expanded to more complicated systems. Our highest level of theory utilized a cubic spline interpolation of a CBS-QCI/CBSB5 potential energy surface mapped at 1° intervals below 35° of inversion and at 5° intervals out to 60°. The kinetic energy terms for the reduced mass $\mu(q)$ and $f_1(q)$ were determined from the MP2/6-311++G** optimized geometries and were fit to eighth-order polynomials in even powers for substitution into the Schrödinger equation. The Numerov−Cooley integration technique was used to solve for the wave functions, providing energy levels in excellent agreement with experimental values for spectroscopic transition of ammonia isotopomers.

The energy difference that appeared in the inversion barrier by expanding to the CBSB5 basis set may indicate that convergence has not yet been reached. This coupled with the sensitivity of the energy levels to the potential energy surface suggests that the largest source of error is the accuracy of the ab initio PES. We find it doubtful that significant improvement will come out of the kinetic terms of the Schrödinger equation. This is heartening given that even better calcualtions of the PES are readily available with the proper commitment of computational resources. Neglect of the $f_1(q)$ kinetic energy term was found to have little effect on the energy levels, but shortcuts in computing the reduced mass function $\mu(q)$ and the PES were shown to introduce significant errors.

Our method is easy to use and can be highly accurate. This study represents a significant advance in our ability to calculate spectroscopic transitions directly from ab initio data. Comparisons with previous calculations indicate superior performance of this method in reproducing the first eight inversional levels of ammonia. The calculations are of sufficient accuracy that they should be useful in helping to assign new transitions for the six ammonia isotopomers, including lines for $^{15}NT_3$, whose inversion transitions have yet to be reported. A modification of this method used to treat amide nitrogen inversion showed utility in the calculation of molecular thermodynamic properties.[44] The results were more robust and accurate than those using conventional approaches and will be addressed in a subsequent paper.

Acknowledgment. We wish to thank Prof. Robert Champion for his assistance with the variable reduced mass adaptation of the Numerov−Cooley integration method, Prof. Guellermo Campoy for a copy of his ammonia program, Dr. Joseph Ochterski for his help with the CBS model chemistries, and Prof. Patrick Vaccaro for numerous helpful discussions and review of the manuscript. This work was supported by the National Institutes of Health.

Supporting Information Available: Calculated energies and inversional kinetic energy terms (7 pages). Ordering information is given on any current masthead page.

References and Notes

(1) Herzberg, G. *Molecular Spectra and Molecular Structure Vol. II., Infrared and Raman Spectra of Polyatomic Molecules*; Van Nostrand Reinhold: New York, 1945.

(2) Lowe, J. P. *Quantum Chemistry*, 2nd ed.; Academic Press: New York, 1993.

(3) Spirko, V. *J. Mol. Spectrosc.* **1983**, *101*, 30.

(4) Spirko, V.; Kraemer, W. P. *J. Mol. Spectrosc.* **1989**, *133*, 331.

(5) (a) Møller, C.; Plesset, M. S. *Phys. Rev.* **1934**, *46*, 618. (b) Pople, J. A.; Binkley, J. S.; Seeger, R. *Int. J. Quantum Chem. Symp.* **1976**, *10*, 1.

(6) Wormer, P. E. S.; Olthof, E. H. T.; Engeln, R. A. H.; Reuss, J. *Chem. Phys.* **1993**, *178*, 189.

(7) Bunker, P. R.; Kraemer, W. P.; Spirko, V. *Can. J. Phys.* **1984**, *62*, 1801.

(8) Campoy, G.; Palma, A.; Sandoval, L. *Int. J. Quantum Chem. Quantum Chem. Symp.* **1989**, *23*, 355.

(9) (a) Petersson, G. A.; Tensfeldt, T. G.; Montgomery, J. A., Jr. *J. Chem. Phys.* **1991**, *94*, 6091. (b) Montgomery, J. A., Jr.; Ochterski, J. W.; Petersson, G. A. *J. Chem. Phys.* **1994**, *107*, 5900.

(10) Janz, G. J. *Thermodynamic Properties of Organic Compounds: Estimation Methods, Principles and Practice*, revised ed.; Academic Press: New York, 1967.

(11) McQuarrie, D. A. *Statistical Thermodynamics*; Harper & Row: New York, 1973.

(12) Atkins, P. W. *Molecular Quantum Mechanics*, 2nd ed.; Oxford University Press: New York, 1983.

(13) Tennyson, J. *J. Chem. Soc., Faraday Trans.* **1992**, *88*, 3271.

(14) Laane, J.; Harthcock, M. A.; Killough, P. M.; Bauman, L. E.; Cooke, J. M. *J. Mol. Spectrosc.* **1982**, *91*, 286.

(15) Durig, J. R.; Zhao, W. *J. Phys. Chem.* **1994**, *98*, 9202.

(16) Laane, J.; Harthcock, M. A. *J. Mol. Spectrosc.* **1982**, *91*, 300.

(17) Press, W. H.; Flannery, B. P.; Teukolsky, S. A.; Vetterling, W. T. *Numerical Recipes: The Art of Scientific Computing*; *FORTRAN Version*; Cambridge University Press: New York, 1990.

(18) Malloy, T. B., Jr. *J. Mol. Spectrosc.* **1972**, *44*, 504.

(19) Irwin, R. M.; Cooke, J. M.; Laane, J. *J. Am. Chem. Soc.* **1977**, *99*, 3273.

(20) Judge, J. H.; Moule, D. C. *J. Mol. Spectrosc.* **1981**, *89*, 276.
(21) Hougen, J. T.; Bunker, P. R.; Johns, J. W. C. *J. Mol. Spec.* **1970**, *34*, 136.
(22) Wilson, E. B., Jr.; Decius, J. C.; Cross, P. C. *Molecular Vibrations: The Theory of Infrared and Raman Vibrational Spectra*; McGraw-Hill: New York, 1955.
(23) Professor Robert Champion, private communication.
(24) Bunker, P. R.; Landesberg, B. M. *J. Mol. Spec.* **1977**, *67*, 374.
(25) Brown, R. D.; Godfrey, P. D.; Kleibömer, B. *J. Mol. Spec.* **1985**, *114*, 257.
(26) Champion, R.; Godfrey, P. D.; Bettens, F. *J. Mol. Spec.* **1992**, *155*, 18.
(27) Cooley, J. W. *Math. Comput.* **1961**, *15*, 363.
(28) Johnson, B. R. *J. Chem. Phys.* **1977**, *67*, 4086.
(29) Algorithm subroutines written by Dr. Bruce R. Johnson, Rice Quantum Institute.
(30) Johnson, B. R. *J. Chem. Phys.* **1978**, *69*, 4678.
(31) Foucrault, M.; Picard, M.; LeClercq, J. M. *Chem. Phys. Lett.* **1989**, *156*, 599.
(32) Ochterski, J. W.; Petersson, G. A.; Wiberg, K. B. *J. Am. Chem. Soc.* **1955**, *117*, 11299.
(33) Curtiss, L. A.; Raghavachari, K.; Trucks, G. W.; Pople, J. A. *J. Chem. Phys.* **1991**, *94*, 7221.
(34) Frisch, M. J.; Trucks, G. W.; Schlegel, H. B.; Gill, P. M. W.; Johnson, B. G.; Robb, M. A.; Cheeseman, J. R.; Keith, T.; Petersson, G. A.; Montgomery, J. A.; Raghavachari, K.; Al-Laham, M. A.; Zakrzewski, V. J.; Ortiz, J. V.; Foresman, J. B.; Cioslowski, J.; Stefanov, B. B.; Nanayakkara, A.; Challacombe, M.; Peng, C. Y.; Ayala, P. Y.; Chen, W.; Wong, M. W.; Andres, J. L.; Replogle, E. S.; Gomperts, R.; Martin, R. L. Fox, D. J.; Binkley, J. S.; Defrees, D. J.; Baker, J.; Stewart, J. P.; Head-Gordon, M.; Gonzalez, C.; Pople, J. A. *Gaussian 95*, Development Version (Revision B.1)); Gaussian, Inc.: Pittsburgh, PA, 1995.
(35) Clark, T.; Chandrasekhar, J.; Spitznagel, G. W.; Schleyer, P. v. R. *J. Comput. Chem.* **1983**, *4*, 294.
(36) Additional calculations at other theory levels not included here.
(37) Chupka, W.; Wiberg, K. B.; Petersson, G. A. To be published.
(38) Morino, Y.; Kuchitsu, K.; Yamamoto, S. *Spectrochim. Acta A* **1968**, *24*, 335.
(39) Marquardt, D. W. *J. Soc. Ind. Appl. Math.* **1963**, *11*, 431.
(40) Kydd, R. A.; Dunham, A. R. C. *J. Mol. Struct.* **1980**, *69*, 79.
(41) Hirota, E.; Sugisaki, R. *J. Mol. Spec.* **1974**, *49*, 251.
(42) Hehre, W.; Radom, L.; Schleyer, P. v. R.; Pople, J. A. *Ab Initio Molecular Orbital Theory*; John Wiley & Sons: New York, 1986.
(43) Campoy, G.; Palma, A. *Int. J. Quantum Chem. Quantum Chem. Symp.* **1986**, *20*, 33.
(44) Wiberg, K. B.; Rablen, P. R.; Rush, D. J.; Keith, T. A. *J. Am. Chem. Soc.* **1995**, *117*, 4261.